Nonlinear fingering dynamics of reaction-diffusion acidity fronts: Self-similar scaling and influence of differential diffusion

D. Lima[a)]
Service de Chimie Physique and Centre for Nonlinear Phenomena and Complex Systems, CP231, Université Libre de Bruxelles, Campus Plaine, 1050 Brussels, Belgium

A. D'Onofrio[b)]
Grupo de Medios Porosos, Departamento de Física, Facultad de Ingenieria, Universidad de Buenos Aires, Paseo Colon 850, (1063) Buenos Aires, Argentina

A. De Wit[c)]
Service de Chimie Physique and Center for Nonlinear Phenomena and Complex Systems, CP231, Université Libre de Bruxelles, Campus Plaine, 1050 Brussels, Belgium

(Received 24 June 2005; accepted 2 November 2005; published online 6 January 2006)

Nonlinear interactions between chemical reactions and buoyancy-driven Rayleigh-Taylor instability of reaction-diffusion acidity fronts of the chlorite-tetrathionate (CT) reaction are studied theoretically in a vertical Hele-Shaw cell or a porous medium. To do so, we perform a numerical integration of a two-variable reaction-diffusion model of the CT system coupled through an advection term to Darcy's law ruling the evolution of the velocity field of the fluid. The fingering dynamics of these chemical fronts is characterized by the appearance of several fingers at onset. These fingers then undergo coarsening and eventually merge to form one single symmetric finger. We study this asymptotic dynamics as a function of the three dimensionless parameters of the problem, i.e., the Damköhler number Da, the diffusivity ratio δ of the two chemical species, and the Rayleigh number Ra constructed here on the basis of the width L_y of the system. For moderate values of Ra, the asymptotic single finger is shown to have self-similar scaling properties while above a given value of Ra, which depends on the other values of the parameters, tip splitting comes into play. Increasing the difference of diffusivities of the two chemical species (i.e., increasing δ) leads to more efficient coarsening and smaller asymptotic fingers. Experimental procedures to verify our predictions are proposed. © *2006 American Institute of Physics*. [DOI: 10.1063/1.2145746]

I. INTRODUCTION

The coupling between autocatalytic chemical reactions and molecular diffusion can lead to the progression of chemical fronts through which a stable steady state invades an unstable one.[1] If the densities of the two corresponding solutions are different, such chemical fronts can become buoyantly unstable if the heavier solution lies on top of the lighter one in the gravity field. Numerous theoretical and experimental works have been devoted to the analysis of such a hydrodynamic instability of chemical fronts both in capillary tubes[2–11] and in Hele-Shaw cells (two glass plates separated by a thin gap width).[11–34] In these latter spatially extended geometries, recent experiments have focused, in particular, on the early times of the instability providing dispersion curves (characterizing the growth rate of the perturbations as a function of their wave number) that have been characterized for two chemical systems, the iodate-arsenous acid[18–21] (IAA) and chlorite-tetrathionate[22–29] (CT) reactions. A comparison between dispersion curves of both reactions[22] shows strong similarities pointing to the fact that in both systems, fingering provides at the onset patterns of analogous wavelength (typically a few millimeters) appearing on the same time scale (of the order of a minute).

Concerning the nonlinear regime, it has been shown numerically that fingering of isothermal IAA (Refs. 13–15 and 31) and CT fronts[22] can lead, after coarsening of several initial fingers, to one single symmetric finger of constant amplitude and velocity. Such a single finger has been characterized quantitatively for a one-variable cubic kinetic scheme modeling the IAA system in the experimental conditions:[31] it is found to be self-similar in spatial units renormalized by the width of the system, the renormalized amplitude scaling as $\mathrm{Da}^{-1/2}$ where Da is the Damköhler number of the problem. Above a given width of the system or given concentration, tip splittings come into play.[31] Recently, similar nonlinear dynamics has also been studied experimentally in the CT reaction:[30] for Hele-Shaw cells of moderate width, several fingers appear at the onset. Following coarsening, those fingers merge and form one single finger. For larger Hele-Shaw cells, where more than a dozen fingers appear at the onset, competition between coarsening and tip splitting has been observed experimentally for both the IAA (Ref. 32) and CT (Ref. 30) reactions. For what concerns the kinetics, the transition to convection as well as the increase of speeds of fronts when convection sets in have been shown

[a)]Electronic mail: dlima@ulb.ac.be
[b)]Electronic mail: adonofr@fi.uba.ar
[c)]Electronic mail: adewit@ulb.ac.be

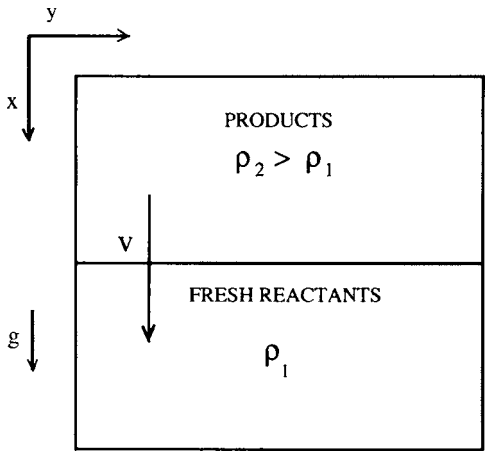

FIG. 1. Sketch of the system.

not to depend significantly on the autocatalysis order for an order greater than 2, this dependence becoming, however, stronger as the systems enter the nonlinear regime.[33,34]

In this framework, it is the objective of this article to investigate how robust the quantitative characteristics of nonlinear fingering of chemical fronts is with regard to the change in kinetics and to study the influence of differential diffusion of the main chemical species on the properties of the nonlinear dynamics. In particular, we perform a detailed quantitative analysis of the nonlinear speed V and mixing zone W of the fingers comparing our results for the CT reaction to those available for the IAA reaction. In order to do so, we perform a numerical integration of a two-variable reaction-diffusion model of the CT reaction coupled through an advection term to Darcy's law ruling the evolution of the flow velocity in a two-dimensional porous medium or Hele-Shaw cell. We show that, as for the IAA reaction,[31] the asymptotic nonlinear dynamics of CT fronts in extended systems are symmetric single self-similar fingers for systems of moderate Ra where Ra is a Rayleigh number constructed upon the width of the system. Above a given Ra, fingers undergo a tip splitting instability. A parametric analysis of the single final finger amplitude W and velocity V is conducted in terms of the important parameters of the problem, i.e., the Rayleigh number Ra, the Damköhler number Da, and the ratio of diffusion coefficients δ of the two main chemical species. As for the IAA kinetics,[31] we recover the self-similar scaling $W/\mathrm{Ra} \sim 1/\sqrt{\mathrm{Da}}$.

The outline of the article is the following. In Secs. II and III, we present the model and the numerical integration technique. The main characteristics of the nonlinear regime are presented in Sec. IV, before a parametric study is undertaken in Sec. V. We end up with discussions in Sec. VI.

II. REACTION-DIFFUSION-ADVECTION EQUATIONS

The system is a two-dimensional porous medium or Hele-Shaw cell filled with the reactants of the CT reaction and of size $L_x \times L_y$ oriented vertically in the gravity field (Fig. 1). When the reaction is triggered at the top of the cell, a chemical front moves downwards invading the fresh reactants, chlorite $[ClO_2^-]$ and tetrathionate $[S_4O_6^{2-}]$ at a reaction-diffusion speed v to yield the main product $[H^+]$ behind it following the overall stoichiometric reaction:[35]

$$7ClO_2^- + 2S_4O_6^{2-} + 6H_2O \rightarrow 7Cl^- + 8SO_4^{2-} + 12H^+. \quad (1)$$

For this reaction, the density of the products, ρ_2, is larger than that of the reactant solution, ρ_1, which yields a buoyantly unstable situation for downward propagating fronts. These fronts undergo then a Rayleigh-Taylor instability producing a density-driven fingering of the self-organized interface.

The CT acid-catalyzed reaction taking place in slight excess of chlorite can be described by a two-variable reaction-diffusion model[36,37] for the two main species of the CT reaction, $\alpha=[S_4O_6^{2-}]$ and $\beta=[H^+]$. These two reaction-diffusion equations are coupled through an advection term to Darcy's law for the evolution of the flow velocity $\underline{u}$. The governing equations for an incompressible solution are then

$$\underline{\nabla} \cdot \underline{u} = 0, \quad (2)$$

$$\underline{\nabla} p = -\frac{\mu}{K}\underline{u} + \rho(\alpha,\beta)\underline{g}, \quad (3)$$

$$\frac{\partial \alpha}{\partial t} + \underline{u} \cdot \underline{\nabla}\alpha = D_\alpha \nabla^2 \alpha - r, \quad (4)$$

$$\frac{\partial \beta}{\partial t} + \underline{u} \cdot \underline{\nabla}\beta = D_\beta \nabla^2 \beta + 6r, \quad (5)$$

with $\underline{\nabla} p$ being the gradient of pressure and where the viscosity μ, the permeability K, and the gravity field $\underline{g}$ are constant in space and time. D_β and D_α are the diffusion coefficients of protons and tetrathionate ions, respectively. The dimensional reaction rate r is given by

$$r = q\{2[ClO_2^-]_0 + 7(\alpha - \alpha_0)\}\alpha\beta^2, \quad (6)$$

where $\alpha_0 \equiv \alpha|_{t=0}$ and q is the reaction rate constant of the overall reaction. In order to avoid possible complexity due to the exothermicity of the reaction,[24,26,27] we consider the system to be isothermal. Changes in the density ρ of the solution occur thus here only through variations of the chemical concentrations of species α and β in the gravity term of Darcy's law (Boussinesq approximation) as

$$\rho(\alpha,\beta) = \rho_0 + \gamma_1\alpha + \gamma_2\beta, \quad (7)$$

where ρ_0 is the density of the solution in the absence of chemical species α and β, while $\gamma_1 = \partial\rho/\partial\alpha|_{\alpha,\beta=0}$ and $\gamma_2 = \partial\rho/\partial\beta|_{\alpha,\beta=0}$. For the CT reaction, downward moving fronts are buoyantly unstable due to an unfavorable density stratification as $\rho_2 > \rho_1$ or $\gamma_2\beta_0 > \gamma_1\alpha_0$, where β_0 is the final product concentration with $\beta_0 = 6\alpha_0$ because of the stoichiometry of the reaction.[22]

Following previous works,[19,22,27,31] we introduce a characteristic velocity $U = \Delta\rho g K/\nu$ where $\Delta\rho = (\rho_2 - \rho_1)/\rho_o$ and $\nu = \mu/\rho_o$ is the kinematic viscosity. We then adimensionalize Eqs. (2)–(5) by scaling velocity, length, and time by U, $L_h = D_\alpha/U$, and $\tau_h = D_\alpha/U^2$, respectively, where L_h and τ_h are the characteristic hydrodynamic length and time scales. Pressure, density, and concentrations α and β are scaled using

$\mu D_\alpha/K$, $(\rho_2-\rho_1)$, and α_0, respectively, while the hydrostatic pressure gradient is incorporated in $\underline{\nabla} p$. The dimensionless Damköhler number, Da, is introduced as the ratio of the hydrodynamic time scale τ_h to the chemical time scale $\tau_c=1/(q\alpha_0^3)$, i.e.,

$$\mathrm{Da}=\frac{\tau_h}{\tau_c}=\frac{D_\alpha}{U^2}q\alpha_0^3. \tag{8}$$

The basic equations for the analysis to follow are then given by

$$\underline{\nabla}\cdot\underline{u}=0, \tag{9}$$

$$\underline{\nabla} p=-\underline{u}+(\gamma_1\alpha+\gamma_2\beta)\underline{i}_x, \tag{10}$$

$$\frac{\partial\alpha}{\partial t}+\underline{u}\cdot\underline{\nabla}\alpha=\nabla^2\alpha-\mathrm{Da}f(\alpha,\beta), \tag{11}$$

$$\frac{\partial\beta}{\partial t}+\underline{u}\cdot\underline{\nabla}\beta=\delta\nabla^2\beta+6\mathrm{Da}f(\alpha,\beta), \tag{12}$$

where

$$f(\alpha,\beta)=\alpha\beta^2(\kappa+7\alpha), \tag{13}$$

with $\kappa=2[\mathrm{ClO}_2^-]_0/\alpha_0-7$ fixed to 1, its typical experimental value,[37] throughout this article. Here, $\delta=D_\beta/D_\alpha$ is the ratio between the diffusion coefficients of the two main species β and α. To avoid any diffusive instabilities,[37–41] we focus here on cases where $\delta\geqslant 1$ which is the experimental situation in the absence of any complexing agent binding the protons. For the special case $\delta=1$, it can be shown[22] that $\beta(x)=6-6\alpha(x)$. The variable β can then be eliminated from the problem and the system reduces to a one-variable (fourth-order) model. Note that, as previously explained in Ref. 22, the coefficients γ_1 and γ_2 are related to each other by the condition $\gamma_1-6\gamma_2=-1$. This is a consequence of the fact that protons β are formed by the reaction in a stoichiometric ratio of 6 is to 1 with respect to the tetrathionate ions α [Eq. (1)].

In the absence of convection ($\underline{u}=0$), the reaction-diffusion system [(11) and (12)] admits traveling front solutions analyzed in detail in Ref. 22. They consist of a front connecting the unstable $(\alpha,\beta)=(1,0)$ solution corresponding to the reactant solution to the stable product solution $(\alpha,\beta)=(0,6)$. This front travels with a reaction-diffusion velocity v which is an increasing function both of δ and Da (explicitly $v\sim\sqrt{\mathrm{Da}}$). The width w of the front defined as the domain in which α takes on values in the interval [0.01,0.99] scales as $\mathrm{Da}^{-1/2}$ while it is an increasing function of δ. In other words, larger Da means sharper fronts traveling faster while larger δ implies more extended fronts with a larger speed due to an increased diffusivity of the autocatalytic species. A linear stability analysis of these fronts with respect to buoyancy-driven hydrodynamic disturbances in the spanwise direction has allowed to obtain dispersion curves[22] which relate the growth rate σ of the disturbances to their wave number k. For isothermal fronts, a band of unstable modes (with positive growth rates) is observed ranging from $k=0$ which is marginally stable to a critical $k=k_c$ beyond which the modes are stable. This band of unstable modes contains a most unstable wave number k_m for which the positive growth rate is maximum. A parametric study has shown the CT fronts to become more unstable with regard to Rayleigh-Taylor fingering when Da is increased or δ decreased.[22] Let us now analyze the quantitative properties of fingering of such CT fronts in the nonlinear regime.

III. NUMERICAL SIMULATIONS OF THE NONLINEAR SYSTEM

To numerically integrate the set of equations [(9)–(13)], we introduce the stream function ψ such that $u=\partial\psi/\partial y$ and $w=-\partial\psi/\partial x$ with $\underline{u}=(u,w)$ the velocity field. Taking the curl of Darcy's law [Eq. (10)] gives

$$\psi_{xx}+\psi_{yy}=\gamma_1\alpha_y+\gamma_2\beta_y, \tag{14}$$

$$\alpha_t+\alpha_x\psi_y-\alpha_y\psi_x=\alpha_{xx}+\alpha_{yy}-\mathrm{Da}\ \alpha\beta^2(\kappa+7\alpha), \tag{15}$$

$$\beta_t+\beta_x\psi_y-\beta_y\psi_x=\delta(\beta_{xx}+\beta_{yy})+6\mathrm{Da}\ \alpha\beta^2(\kappa+7\alpha), \tag{16}$$

where the subscripts indicate partial derivatives. We numerically solve Eqs. (14)–(16) using a pseudospectral method[22,31,42,43] on a two-dimensional domain of dimensionless width L_y' and length L_x'. We note that the dimensionless width $L_y'=L_y/L_h$ corresponds to the Rayleigh number

$$\mathrm{Ra}=\frac{L_y}{L_h}=\frac{\Delta\rho g K L_y}{\nu D_\alpha}, \tag{17}$$

constructed using the permeability K of the porous medium (equal to $a^2/12$ in a Hele-Shaw cell of gapwidth a), the kinematic viscosity ν, and the width L_y of the system. If we define the aspect ratio as $A=L_x/L_y$ we obtain $L_x'=A\mathrm{Ra}$. Experimentally, Ra can be varied by changing the concentrations (and hence $\Delta\rho$) or the permeability K. The simplest way, however, is to vary it by changing the width L_y of the system, as has been done experimentally recently.[26]

Our numerical scheme, adapted from Ref. 42 and used successfully previously[22,27,31] to take chemical reactions into account, is based on Fourier expansions for the stream function ψ and concentrations α and β with periodic boundary conditions in both directions. To deal with periodicity in the x direction, we start with $\alpha=0$ and $\beta=6$ at the top ($x=0$) of the cell and switch to $\alpha=1$ and $\beta=0$ at $x=0.05L_x'$. The reverse switch of α from 0 to 1 and of β from 0 to 6, applied at the bottom $x=0.95L_x'$, on the contrary corresponds to a heavier solution invading upwards the lighter reactants which is a buoyantly stable situation. Random white noise of 0.2% maximum amplitude is applied at the front. To test the accuracy of the numerical code, we have checked that we reproduce the reaction-diffusion profiles obtained in Ref. 22 by another method. Moreover, the properties of the fingers at the onset (initial wavelength and time of appearance) are in good quantitative agreement with the ones predicted by the linear stability analysis.[22] In addition, the nonlinear properties of the fingers such as the final length of asymptotic single fingers and the parameters above which tip splittings occur (see section below) have been checked to be robust with regard to the refinement of time and space discretiza-

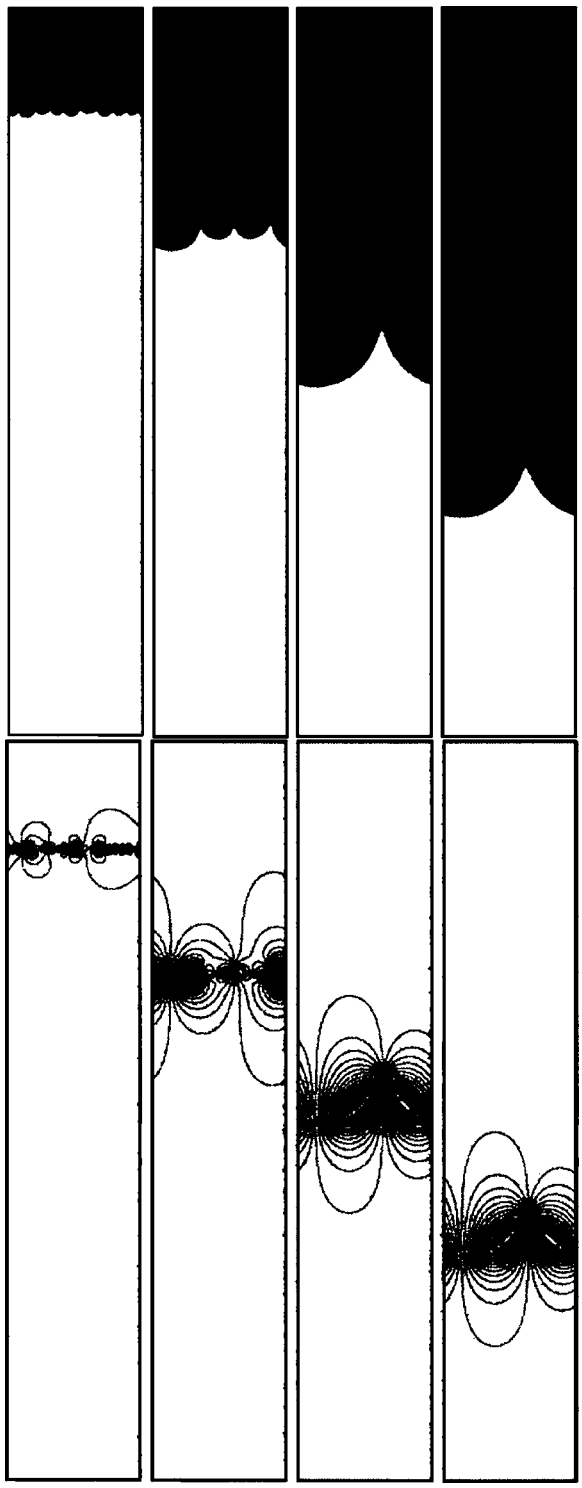

FIG. 2. Density fingering of a CT front traveling downwards and shown at times $t=420$, 1020, 1620, 2220 (from left to right) for Ra=512, $\delta=1$, and Da=0.004. The upper and lower panels show the concentration and stream function fields, respectively.

tions steps. All simulations presented here use typically a time step $dt=0.2$ and a spatial step $dx=dy=4$. For each simulation, we check that the Courant-Friedrichs-Lewy (CFL) stability criterion[44] ($|u_{\max}|dt/dx \leqslant 1$ where $|u_{\max}|$ is the maximum fluid velocity in the integration domain) is always verified throughout the numerical integration. Typically, for the results of Fig. 2, $|u_{\max}|=0.923$ in the asymptotic regime giving a CFL condition equal to 0.05 which ensures stability of the code. Throughout this article, the density plots of the concentrations are zoomed on the unstable front propagating downward and show the product of the reaction in black and the fresh reactants in white. In other words, we present the concentration α of the reactant in the downward moving front on a gray scale ranging from $\alpha=0$ (black) to $\alpha=1$ (white). Let us note that the velocity fields in the convection rolls surrounding the front typically extend on a larger scale than the reactive zone. In this regard, we always ensure that the dynamics presented in the various figures are occurring far from the boundaries of our integration domain. In other words, the dynamics such as the one presented on Fig. 2 is shown as a zoom on a much longer integration domain.

IV. NONLINEAR DYNAMICS

Figure 2 shows a typical nonlinear evolution of the hydrodynamically unstable front traveling downwards in the gravity field in a spatially extended system with Ra=512. At the onset, roughly nine fingers appear characterized by a wavelength in good agreement with the one predicted by the linear stability analysis.[22] In the course of time, these fingers merge in a coarsening dynamics typical of fingering phenomena.[45] The corresponding stream function shows that, as for pure hydrodynamic fingering,[42] unequal crossflow causes dominating fingers to spread and shield their neighbors which leads to a decrease in time of the total number of fingers. Eventually, the asymptotic dynamics is one single symmetric finger traveling without any further deformation at a constant velocity $V>v$, where v is the dimensionless reaction-diffusion front velocity. The main difference with pure hydrodynamic fingering which can ultimately feature a long finger which continues to stretch in time is that, here, chemistry favors planar fronts which leads to a final constant length of the mixing zone. This coarsening evolution of several initial reactive fingers towards one single symmetric finger has already been described in numerical studies of the IAA (Refs. 14 and 31) and CT reactions[22] as well as in the experiments in Hele-Shaw cells with the CT system.[30] In this later work, the same dynamics as the one depicted in Fig. 2 has been experimentally observed with the CT reaction. It is here our goal to analyze this nonlinear dynamics quantitatively.

Let us first study the properties of the asymptotic single finger as a function of the Damköhler number Da. The linear stability analysis of the problem shows that increasing Da leads to more unstable fronts characterized in the linear regime by a larger most unstable wave number k_m with the largest growth rate.[22] Numerical simulations of the full nonlinear system confirm this tendency, as shown in Fig. 3, where fixing Ra=512 and $\delta=1$, we compare the nonlinear dynamics of fingers for two different values of Da. For Da =0.004 (right column), fingers appear earlier with a smaller wavelength and, later on, merge quicker than in the case of Da=0.001 (left column). These tendencies can also be examined, thanks to the measure of the mixing length L_d, defined as the distance between the tip and the rear of the fingers,

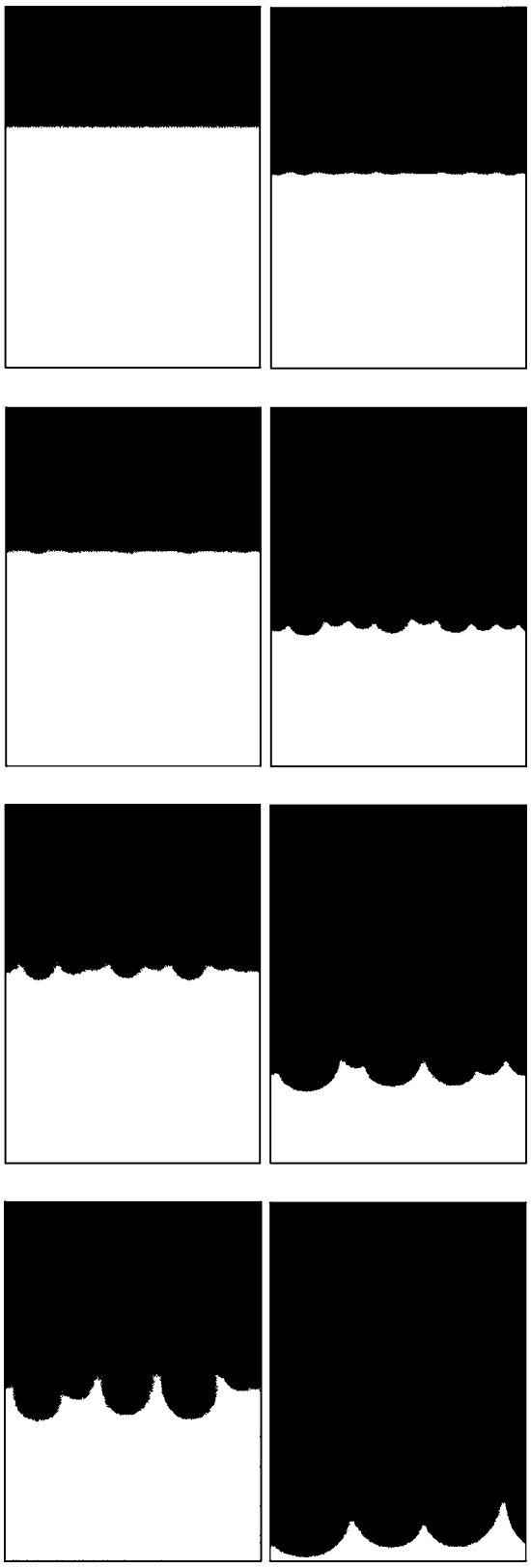

FIG. 3. Fingering of CT fronts for Da=0.001 (first column) and Da =0.004 (second column) shown at times t=300, 460, 600, 760 from top to bottom with Ra=512 and δ=1.

which are chosen here as the location along the x axis in front of and behind which the transversely averaged concentration $\langle \alpha(x,t) \rangle$ is, respectively, larger than 0.99 and smaller than 0.01.[31] Figure 4 shows the mixing length versus time for

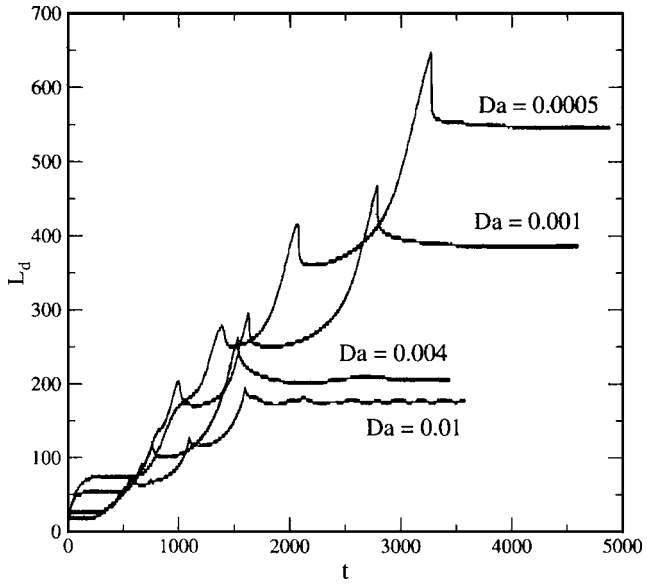

FIG. 4. Mixing length L_d vs time for Ra=512, δ=1, and different values of Da.

Ra=512, δ=1, and four different values of Da. Starting from a step function of zero mixing length, the system relaxes in the beginning towards the pure reaction-diffusion front characterized by a constant width w, which is a decreasing function of Da. After a given induction time which decreases with Da, fingering sets in characterized by a linear growth of the mixing length with a slope that increases with Da. Coarsening due to merging of fingers can be seen through the occurrence of bumps in the temporal dependence of the mixing zone. After a given time, all fingers merge into one single finger of constant mixing zone, as witnessed by the final plateau in Fig. 4. This asymptotic constant value of L_d, which we note W, is nothing else than the longitudinal extent of the mixing zone or also the length of the final asymptotic finger. For larger Da, hence more unstable systems, the coarsening takes less time, eventually leading to a single finger of smaller length W. It is here useful to recall that the Damköhler number Da is the ratio between the hydrodynamic and chemical time scales. A large value of Da means a more effective chemistry. Let us moreover recall that pure reaction-diffusion systems feature planar fronts as long as diffusive instabilities are not present, which is the case here for our two-variable model as we consider only $\delta \geqslant 1$. Hence increasing Da, i.e., the role of chemistry will favor the tendency towards planar fronts which, in the nonlinear fingering regime, means more effective coarsening and asympotic fingers of smaller length W.

These tendencies, obtained with the two-variable CT model for a value of δ=1, are analogous to those observed in numerical simulations of fingering of the one-variable (third-order) IAA model.[31] This is not surprising as, for δ=1, the two-variable model [(11) and (12)] can be simplified into a one-variable (fourth-order) model for the CT reaction[22] while Coroian and Vasquez[34] have shown that the nonlinear speed of fingers of chemical fronts is almost independent on the order of the reaction term for one-variable models of order of the autocatalysis larger than 2.

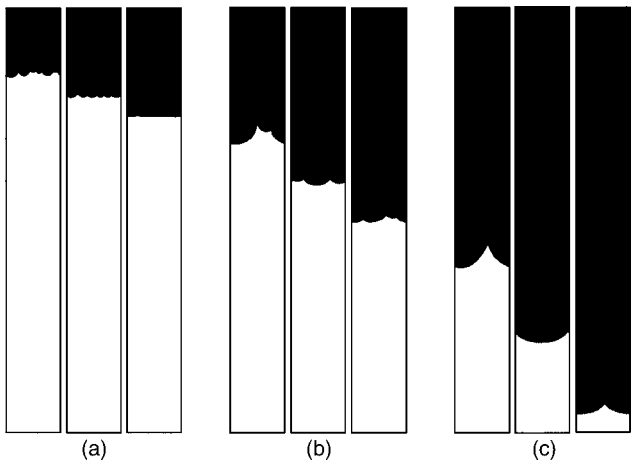

FIG. 5. Nonlinear coarsening dynamics towards one single finger for Ra $=768$, Da$=0.005$, and three different values of δ, i.e., $\delta=1$, 2, and 3 from left to right shown at times $t=1000$ (a), $t=2000$ (b), and $t=3800$ (c).

However, in aqueous solutions of CT reactants, δ is likely to be equal to 3 or even more as protons diffuse probably at least three times faster than tetrathionate ions.[46] If $\delta \neq 1$, we must then keep the full two-variable model. Let us therefore analyze the influence of differential diffusion with $\delta > 1$ on the nonlinear density fingering dynamics of CT fronts. Figure 5 compares fingering for increasing values of δ (left to right), for Ra$=768$, and Da$=0.005$ at three successive times. Figure 6 shows the corresponding mixing lengths L_d as a function of time. For $\delta=1$, the front is sharper than for $\delta=3$, for instance, hence the same density difference acts across a less extended front width which leads to a more unstable system.[22] Fingering starts then earlier with a smaller wavelength for $\delta=1$. At $t=1000$ [Fig. 5(a)], fingers are indeed more developed and have a smaller wavelength for $\delta=1$ than for $\delta=2$ or 3. Once fingering starts, the system with larger δ does not take long to reach the single finger dynamics. This is due to the fact that the width of the band of unstable modes decreases as δ increases.[22] The system must cover less merging steps before reaching the asymptotic finger. Therefore, even though fingering starts later, it takes roughly the same time to get to the single finger configuration. Coarsening takes place until the system reaches the final single finger state. This finger travels with constant velocity and mixing length (Fig. 6). Once the asymptotic finger develops, the one corresponding to a larger δ has a shorter mixing length. This can be understood as $\delta > 1$ means that the activator (protons) diffuse faster than the inhibitor (tetrathionate ions). The front velocity, thus, as one would intuitively expect, increases with δ, and this means that the fingers are entrained by the front. This effect hinders the fingers development and leads to a final asymptotic finger of smaller length W.

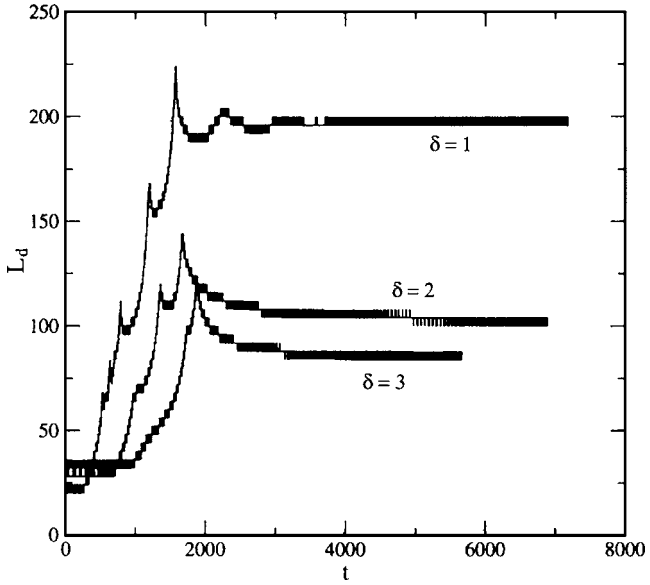

FIG. 6. Mixing length L_d vs time for Ra$=768$, Da$=0.005$, and different values of δ, i.e., for the simulations of Fig. 5.

V. PARAMETRIC STUDY

The nonlinear fingering dynamics presented in the preceding section features several fingers at the onset followed by a coarsening leading eventually to one single asymptotic finger traveling with a fixed shape of length W at a constant nonlinear speed V larger than that of the pure reaction-diffusion front speed v. Let us analyze here the properties of this asymptotic finger as a function of the various parameters of the problem, i.e., the Rayleigh number Ra, the Damköhler number Da, the density expansion coefficients γ_1 and γ_2, as well as the diffusivity ratio δ.

First of all, let us note that our numerical simulations show that the properties of the density fingers are independent of the values of γ_1 and γ_2, as long as the relation $\gamma_1 - 6\gamma_2 = -1$ imposed by the stoichiometry of the reaction[22] is respected. Varying these density coefficients, but keeping the later relation and all the other parameters unchanged, leads to the same fingering phenomenon. In other words, for the same initial conditions, the nonlinear pattern is the same. In that respect, all simulations shown in this article have been obtained for $\gamma_1=1.28$ and $\gamma_2=0.38$.

A. Self-similar scaling versus tip splitting

In the asymptotic single finger dynamics, the rear and tip of the finger travel in parallel at a speed V, separated by a constant mixing zone of extent W. In Figs. 7 and 8, we plot the length W and speed V, respectively, as a function of Da for different values of Ra. For a given Da, the mixing zone W and speed V both increase with the Rayleigh number. On the other hand, for a fixed Ra, W is inversely proportional to $\sqrt{\text{Da}}$ while V increases with Da. Increasing Da can be obtained experimentally by increasing the initial concentration of tetrathionate ions. Our result agrees thus with those of Bánsági *et al.*[26] who experimentally found that the speed of fingers V increases with this initial concentration. Examining Figs. 7 and 8 together one can see that by increasing Da, i.e., the ratio between the hydrodynamic and chemical time scales, one thus obtains less elongated but faster moving single fingers. A greater Da means that the chemistry (which favors planar fronts) is more effective; thus it opposes the hydrodynamic Rayleigh-Taylor instability more efficiently. Indeed, the effect of the presence of chemistry is clear when

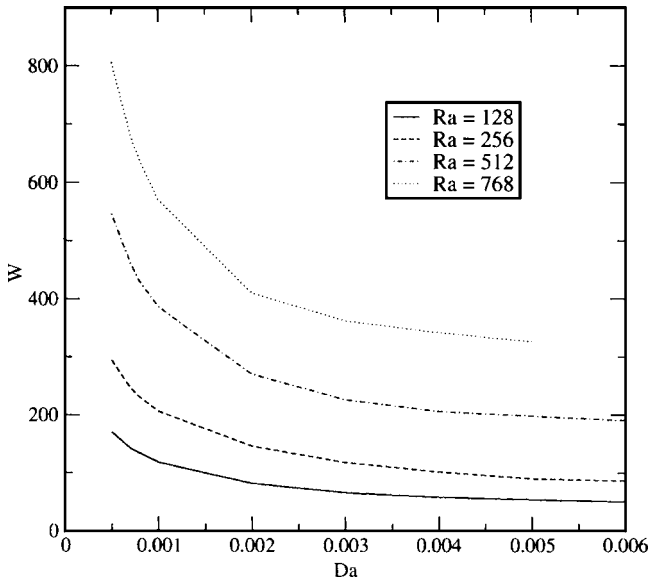

FIG. 7. Length W of the single asymptotic finger as a function of Da for different values of Ra and $\delta=1$. For Ra=768, finger splitting occurs for $\mathrm{Da}\geqslant 0.005$.

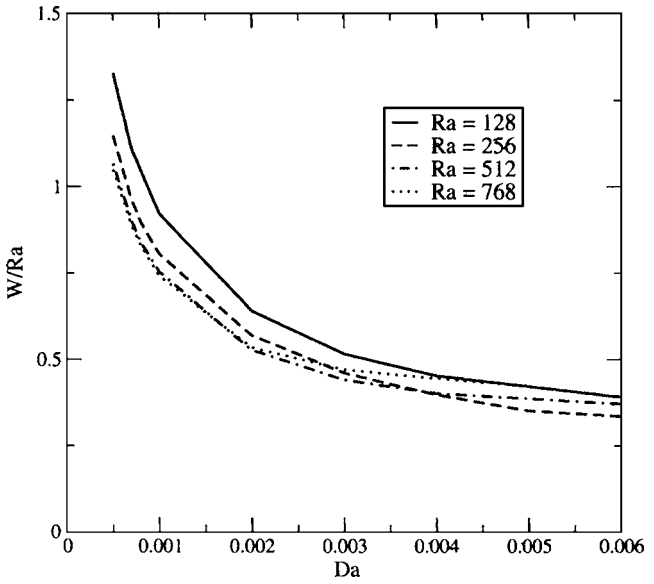

FIG. 9. Length W of the single asymptotic finger divided by the Rayleigh number Ra as a function of Da for $\delta=1$ and four different values of Ra. In this scaling, all curves of Fig. 8 are collapsing into one curve which follows the trend $W/\mathrm{Ra}=0.03/\sqrt{\mathrm{Da}}$.

observing the way W varies for small Da. The introduction of chemistry (small Da) leads to a dramatic change in the length of the asymptotic finger. Further changes in Da, however, do not change appreciably W. After a certain value of the Damköhler number, chemistry opposes efficiently the convective rolls and increasing Da only leads to small changes on W. The dependence of the properties of the fingers on Ra can be understood typically if Ra is varied by changing the width L_y of the cell. This allows more fingers to appear at the onset and longer convective rolls to develop. This leads for a fixed set of chemical concentrations (i.e., fixed Da) to longer fingers traveling faster.

We have plotted W/Ra, i.e., the dimensionless length W of the asymptotic finger scaled by Ra vs Da for $\delta=1$ in Fig. 9. We find that all curves tend towards the same curve which follows the law $W/\mathrm{Ra}=0.03/\sqrt{\mathrm{Da}}$, suggesting a self-similar behavior. This result is analogous to the one obtained previously on a one-variable model of the IAA reaction.[31] To check that the asymptotic fingers for different values of Ra are self-similar, we plot in Fig. 10 the normalized longitudinally averaged asymptotic concentration profile $\langle c(y)\rangle$ as a function of the width of the system normalized by Ra. To do so, for every value of y $(0\leqslant y\leqslant L_y)$ we calculate the arithmetic averaged concentration $\langle c(y)\rangle$ which gives us the finger profile averaged along the longitudinal coordinate. Extracting the maximum and minimum values of this averaged

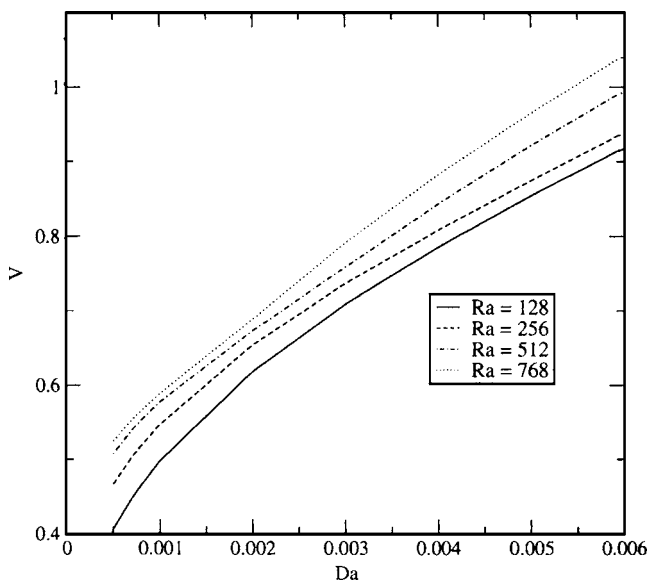

FIG. 8. Velocity V of the asymptotic single finger as a function of Da for various values of Ra and $\delta=1$. This reaction-diffusion-convection velocity V is larger than the pure reaction-diffusion velocity v of the chemical front.

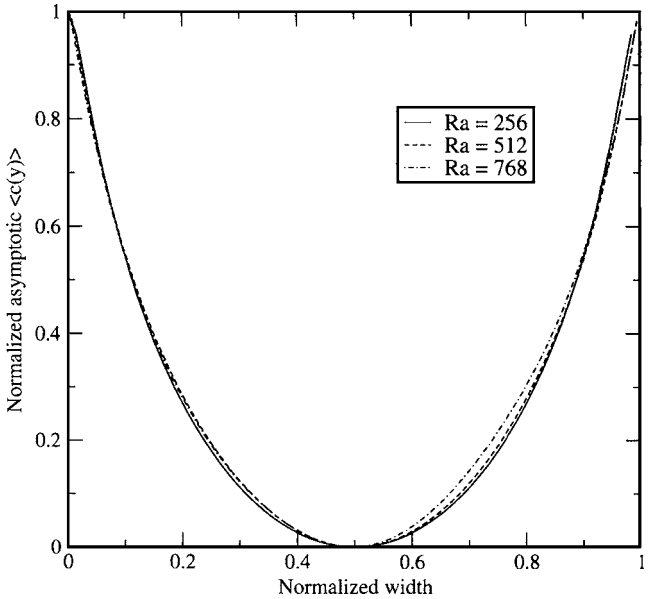

FIG. 10. Normalized profiles of the asymptotic fingers for different values of Ra, Da=0.005, and $\delta=1$. All profiles collapse onto one self-similar profile.

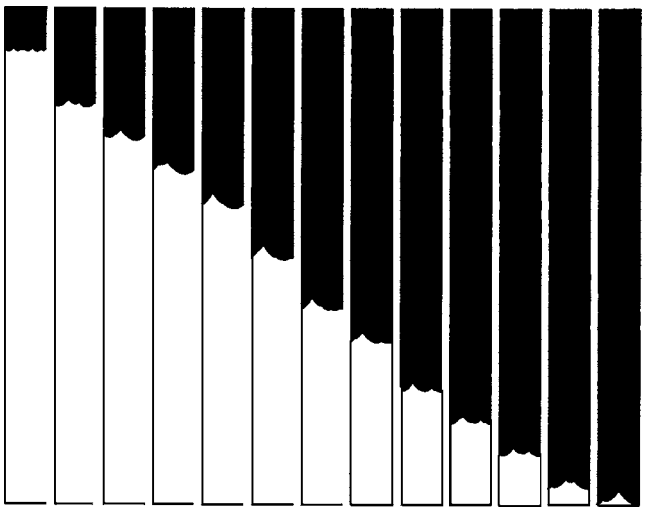

FIG. 11. Nonlinear fingering dynamics featuring competition between coarsening and tip splittings for Ra=768, Da=0.015, and $\delta=1$. For these values of Ra and δ, finger splitting occurs for Da$\geqslant$0.005. The dynamics is shown here at successive times $t=500$, 1200, 1600, 2000, 2400, 3000, 3600, 4000, 4600, 5000, 5400, 5800, 5980.

profile, we compute its amplitude. This amplitude is used to normalize the averaged profile $\langle c(y)\rangle$ between 0 and 1. The transverse coordinate y scales in our dimensionless units between 0 and Ra. We plot then the normalized asymptotic $\langle c(y)\rangle$ on a normalized width, i.e., in units $y'=y/\mathrm{Ra}$. As can be seen on Fig. 5(c), the transverse location of the tip of the fingers depends upon the initial condition. We therefore translate the asymptotic profile along y' to superpose all the tips at the position $y'=1/2$. This procedure shows in Fig. 10 that all profiles collapse into one single self-similar solution independently of the value of Ra. This self-similar profile is strikingly analogous to the one computed for fingering of the IAA reaction.[31] This suggests that this self-similarity is independent of the chemistry involved. It means also that, if fingering of chemical fronts is observed in a system of which we double the value of Ra, it produces a finger that will be twice as long. This can be achieved either by taking a width of the porous medium or Hele-Shaw cell twice as large (this doubles L_y) or by changing the gapwidth of the cell or also the density ratio (by varying concentrations, for instance). Moreover, the same profile seems to be obtained for both order 3 (IAA) and 4 (CT) autocatalysis.

This self-similar scaling occurs in a given domain bounded in the (Ra, Da) plane. Indeed, we observe that for a fixed Da, there is a critical Ra above which finger splitting comes into play and destroys the single finger. Similarly, for a fixed Ra, tips splitting becomes operative above a critical value of Da. For Ra=768, for instance, we have observed the phenomenon of finger splitting for Da$>$0.005 which translates in Fig. 7 by the fact that the curve W as function of Da is interrupted above Da=0.005. The greater Da, the more important finger splitting becomes. This can be understood as, for larger Da, chemistry is more active leading to sharper fronts. Sharper interfaces is known in the pure hydrodynamic fingering instabilities to favor tip splitting phenomena.[42,45] Figure 11 shows an example of nonlinear finger splittings for Ra=768, Da=0.015, and $\delta=1$. After the development of the first fingers, coarsening takes place and the asymptotic finger is reached after some time. But instead of keeping its shape, as it is the case for lower values of Da, the single finger tip undergoes a splitting that starts as a dent and becomes more and more pronounced. The fingers so created will eventually merge again, leading once more to one single finger. A dent appears and the splitting-coarsening dynamics reappears. A parallel closer look at the concentration and stream function fields (Fig. 12) shows that the velocity field dynamics is the same as that previously analyzed by Tan and Homsy[42] in viscous fingering tip splitting events. If the finger front has spread wide enough to allow more than two new wavelengths of the instability to grow and if, in addition, the concentration gradient at the finger tip becomes steep enough (which causes the growth rate of the disturbance to increase), the spreading finger becomes unstable and splits into more fingers. In that respect, it can be understood that, for a fixed Da, splitting comes into play above a given Ra. Either Ra is increased by using larger L_y; in that case, the final finger can become large enough to allow the instability to operate again and lead to splitting. Or Ra can be increased by implying a

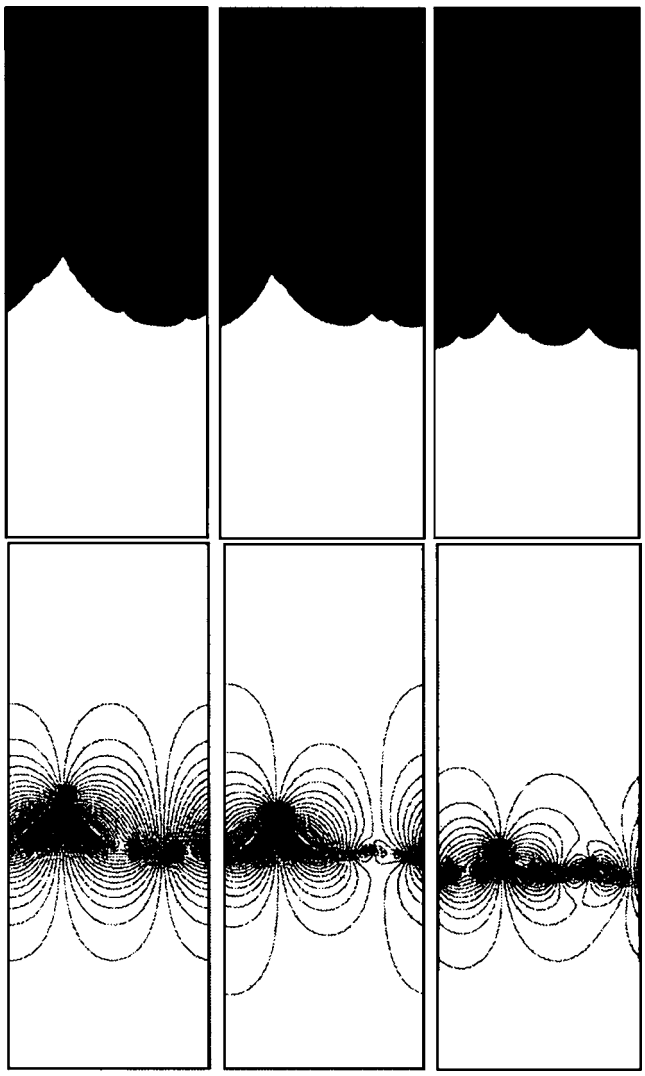

FIG. 12. Concentration and stream function fields for Ra=768, Da=0.015, and $\delta=1$. The dynamics is shown here at successive times $t=3000$, 4200, 4800.

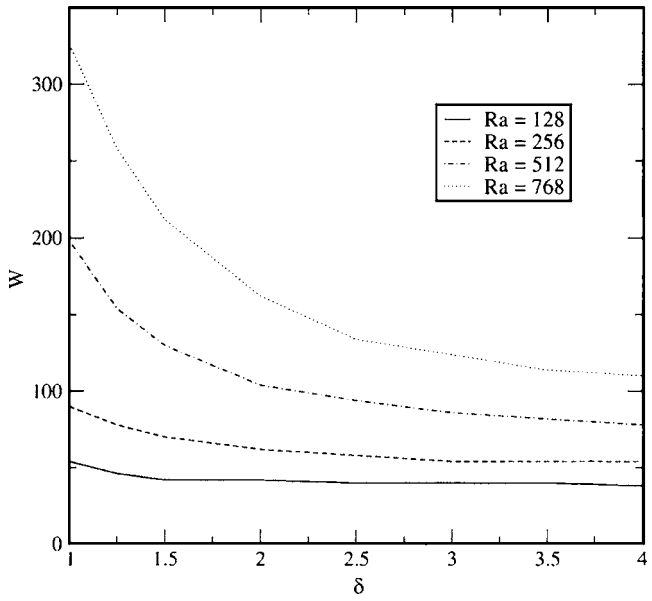

FIG. 13. Length W of the single asymptotic finger as a function of δ for different values of Ra and Da=0.005.

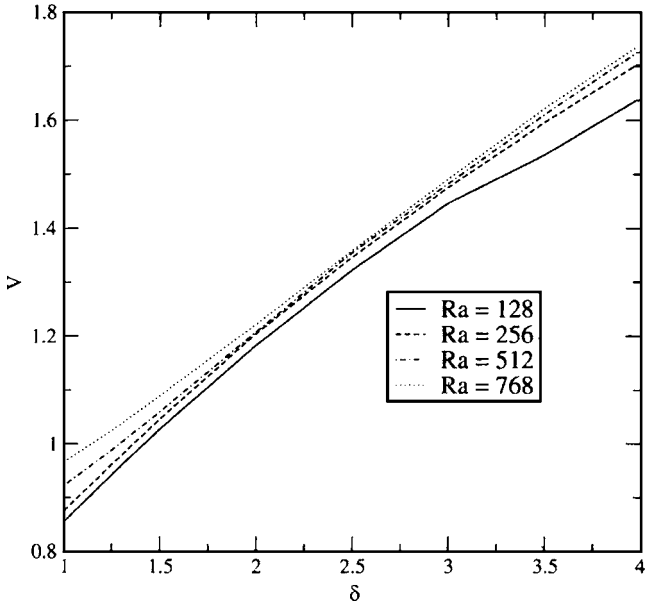

FIG. 14. Velocity V of the asymptotic single finger as a function of δ for various values of Ra and Da=0.005.

larger $\Delta\rho$ across the front in which case the front of the finger becomes also more unstable. A similar interpretation explains why, for a fixed Ra, splitting appears above a given critical Da. Increasing Da leads to sharper fronts[22] which favors the steepening needed for splitting.

B. Influence of differential diffusion

The preceding self-similar scaling has been characterized for $\delta=1$. Let us now analyze what is the influence of differential diffusion of the two main chemical species α and β of the problem onto the nonlinear dynamics. When $\delta>1$, the nonlinear dynamics also evolves towards one single finger as seen on Fig. 5, the coarsening being more efficient for increasing values of this parameter. The final length W of the single finger is a decreasing function of δ, as can be seen on Fig. 13, which plots W as a function of δ for different values of Ra.

For fixed δ, increasing Ra leads to a larger asymptotic finger. On the other hand, for Ra=128 the length of the asymptotic finger is almost independent of δ while the change of W with δ is much more dramatic for larger Ra. Above $\delta=3$, the length of the fingers tend to saturate for all Ra. However, for larger systems (Ra=768), $\delta>3.5$ leads to finger splitting analogous to the one discussed above for the case of large Da. The velocities of these asymptotic fingers increase with δ (Fig. 14) which is related to the increase of the speed of the underlying reaction-diffusion front with δ. Eventually, it is striking to realize that the self-similarity of the asymptotic fingers can also be recovered independently of δ. Indeed, as Fig. 15 is attesting, the same profiles as that of Fig. 10 are recovered for various values of Ra and δ.

VI. CONCLUSIONS

We have investigated here the nonlinear dynamics of the fingering of CT fronts taking place in a porous medium or a Hele-Shaw cell for downward moving fronts as heavy products are formed on top of lighter fresh reactants. The initial fingers merge to form one single symmetric asymptotic finger which is found to be self-similar. This is an interesting result, because the self-similar trend $W/\mathrm{Ra}\sim 1/\sqrt{\mathrm{Da}}$ as well as the normalized asymptotic profiles are analogous to those previously obtained in the study of the nonlinear dynamics of fingering for the IAA reaction.[31] So, this self-similarity behavior seems to be the same for both order 3 and 4 kinetics giving rise to the reaction front. Another similarity between fingering in the IAA and the CT reactions is the existence of finger splitting for larger Damköhler numbers and larger values of Ra. We have also shown that differential diffusion plays an important role on the nonlinear fingering dynamics

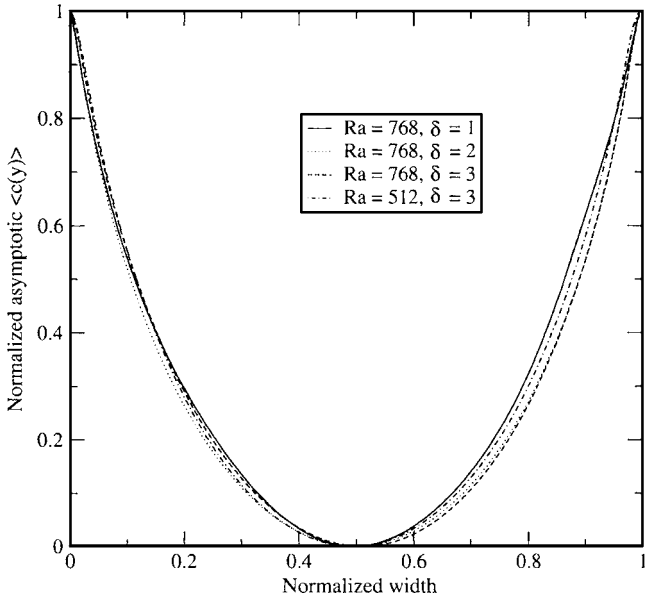

FIG. 15. Normalized profiles of the asymptotic fingers for different values of δ and Ra for Da=0.005. The profiles are those of the fingers in Fig. 5(c). All profiles collapse into one self-similar profile identical to that of Fig. 10.

of chemical fronts. Chemical fronts travel faster in systems where the products (activator species) experience faster diffusion than the reactants (inhibitor species). Larger δ also yields longer induction time of the instability. The self-similar normalized asymptotic profiles of the fingers are, however, independent of δ.

This work calls for future works in various directions. First of all, it would be very nice to compare our predictions with the experimental results. We have analyzed here among others the influence of differential diffusion of the chemical species on the nonlinear dynamics. This influence could be checked for in experiments by using complexing agents binding one of the main chemical species of the autocatalytic scheme and hence altering their diffusivity.[37,40,41] Furthermore, additional experimental work on the quantitative characterization of the full nonlinear dynamics in spatially extended systems is needed. A coarsening dynamics from several initial fingers towards one single symmetric finger has already been observed experimentally in the CT system.[26] Further quantitative experimental analysis of the conditions of stability of this symmetric finger, of the influence of the boundaries of the experimental reactor, as well as of the details of the flow field and of the competition with tip splittings[26,32] would be welcome both for IAA and CT fronts. A parametric study of the length W of the asymptotic finger as a function of the permeability of the porous medium, of the gapwidth of a Hele-Shaw cell, or of concentrations (i.e., varying Da) for various values of the width of the reactor (and hence of Ra) might give further insights into the experimental validation of the self-similar scaling $W/\mathrm{Ra} \sim 1/\sqrt{\mathrm{Da}}$ that we have uncovered numerically for both CT and IAA fronts. A more firm mathematical understanding of the origin of this self-similar scaling would also be particularly elegant.

From both experimental and theoretical perspectives, it would be interesting to also understand the influence of the kinetics of the reaction and of differential diffusion on the self-similar scaling and the nonlinear properties of the system. We have shown that the dynamics of the one-variable third-order IAA (Ref. 31) and fourth-order CT models obtained when all chemical species have the same diffusion coefficients seems to be analogous. In the same spirit, Vasquez and co-workers have shown that the onset of convection and nonlinear speed of convective chemical fronts seem to be independent of the order of the autocatalysis for orders larger than 2, the fronts with kinetics of order 2 being, however, characterized by different nonlinear speeds and thresholds of instability.[33,34] Further understanding of the origin of such discrepancy between orders 2 and larger than 2 should be looked for. Eventually, theoretical analysis of the robustness of our results with regard to changes in the hydrodynamic description and the incorporation of heat effects might be undertaken in the future.

ACKNOWLEDGMENTS

We wish to thank CONICET (Argentina), FNRS (Belgium), and the Prodex programme (Belgium) of ESA for financial support.

[1] W. van Saarloos, Phys. Rep. **386**, 29 (2003).
[2] I. R. Epstein and J. A. Pojman, *An Introduction to Nonlinear Dynamics: Oscillations, Waves, Patterns and Chaos* (Oxford University Press, New York, 1998).
[3] I. Nagypál, G. Bazsa, and I. R. Epstein, J. Am. Chem. Soc. **108**, 3635 (1986).
[4] I. Nagypál and I. R. Epstein, J. Phys. Chem. **94**, 4966 (1990).
[5] J. A. Pojman and I. R. Epstein, J. Phys. Chem. **95**, 1299 (1991).
[6] J. A. Pojman, I. R. Epstein, T. J. McManus, and K. Showalter, J. Phys. Chem. **95**, 1299 (1991).
[7] J. Masere, D. A. Vasquez, B. F. Edwards, J. W. Wilder, and K. Showalter, J. Phys. Chem. **98**, 6505 (1994).
[8] B. F. Edwards, J. W. Wilder, and K. Showalter, Phys. Rev. A **43**, 749 (1991).
[9] D. A. Vasquez, J. W. Wilder, and B. F. Edwards, J. Chem. Phys. **98**, 2138 (1993).
[10] D. A. Vasquez, J. M. Littley, J. W. Wilder, and B. F. Edwards, Phys. Rev. E **50**, 280 (1994).
[11] J. A. Pojman, I. P. Nagy, and I. R. Epstein, J. Phys. Chem. **95**, 1306 (1991).
[12] J. Huang, D. A. Vasquez, B. F. Edwards, and P. Kolodner, Phys. Rev. E **48**, 4378 (1993).
[13] Y. Wu, D. A. Vasquez, J. W. Wilder, and B. F. Edwards, Phys. Rev. E **52**, 6175 (1995).
[14] J. Huang and B. F. Edwards, Phys. Rev. E **54**, 2620 (1996).
[15] D. A. Vasquez, J. W. Wilder, and B. F. Edwards, J. Chem. Phys. **104**, 9926 (1996).
[16] D. A. Vasquez and C. Lengacher, Phys. Rev. E **58**, 6865 (1998).
[17] M. R. Carey, S. W. Morris, and P. Kolodner, Phys. Rev. E **53**, 6012 (1996).
[18] M. Böckmann and S. C. Müller, Phys. Rev. Lett. **85**, 2506 (2000).
[19] A. De Wit, Phys. Rev. Lett. **87**, 054502 (2001).
[20] J. Martin, N. Rakotomalala, D. Salin, M. Böckmann, and S. C. Müller, J. Phys. IV **11**, Pr6-99 (2001).
[21] J. Martin, N. Rakotomalala, D. Salin, and M. Böckmann, Phys. Rev. E **65**, 051605 (2002).
[22] J. Yang, A. D'Onofrio, S. Kalliadasis, and A. De Wit, J. Chem. Phys. **117**, 9395 (2002).
[23] D. Horváth, T. Bánsági, Jr., and A. Tóth, J. Chem. Phys. **117**, 4399 (2002).
[24] T. Bánsági, Jr., D. Horváth, Á. Tóth, J. Yang, S. Kalliadasis, and A. De Wit, Phys. Rev. E **68**, 055301 (2003).
[25] T. Bánsági, Jr., D. Horváth, and Á. Tóth, Phys. Rev. E **68**, 026303 (2003).
[26] T. Bánsági, Jr., D. Horváth, and Á. Tóth, Chem. Phys. Lett. **384**, 153 (2004).
[27] S. Kalliadasis, J. Yang, and A. De Wit, Phys. Fluids **16**, 1395 (2004).
[28] D. A. Vasquez and A. De Wit, J. Chem. Phys. **121**, 935 (2004).
[29] T. Rica, D. Horváth, and Á. Tóth, Chem. Phys. Lett. **408**, 422 (2005).
[30] T. Bánsági, Jr., D. Horváth, and Á. Tóth, J. Chem. Phys. **121**, 11912 (2004).
[31] A. De Wit, Phys. Fluids **16**, 163 (2004).
[32] M. Böckmann and S. C. Müller, Phys. Rev. E **70**, 046302 (2004).
[33] D. A. Vasquez and E. Thoreson, Chaos **12**, 49 (2002).
[34] D. I. Coroian and D. A. Vasquez, J. Chem. Phys. **119**, 3354 (2003).
[35] I. Nagypál and I. R. Epstein, J. Phys. Chem. **90**, 6285 (1986).
[36] A. Tóth, D. Horváth, and A. Siska, J. Chem. Soc., Faraday Trans. **93**, 73 (1997).
[37] D. Horváth and A. Tóth, J. Chem. Phys. **108**, 1447 (1998).
[38] Y. Kuramoto, *Chemical Oscillations, Waves and Turbulence* (Springer-Verlag, Berlin, 1984).
[39] D. Horváth, V. Petrov, S. K. Scott, and K. Showalter, J. Chem. Phys. **98**, 6322 (1993).
[40] D. Horváth and K. Showalter, J. Chem. Phys. **102**, 2471 (1995).
[41] A. Tóth, I. Lagzi, and D. Horváth, J. Phys. Chem. **100**, 14837 (1996).
[42] C. T. Tan and G. M. Homsy, Phys. Fluids **31**, 1330 (1988).
[43] A. De Wit and G. M. Homsy, J. Chem. Phys. **110**, 8663 (1999).
[44] W. H. Press, S. A. Teukolsky, W. T. Vetterling, and B. P. Flannery, *Numerical Recipes in C*, (Cambridge University Press, Cambridge, 1988).
[45] G. M. Homsy, Annu. Rev. Fluid Mech. **19**, 271 (1987).
[46] M. Fuentes, M. N. Kuperman, and P. De Kepper, J. Phys. Chem. A **105**, 6769 (2001).